Binding between endohedral Na atoms in Si clathrate I; a first principles study

2008 J. Phys.: Condens. Matter 20 385209

(http://iopscience.iop.org/0953-8984/20/38/385209)

J. Phys.: Condens. Matter **20** (2008) 385209 (6pp) doi:10.1088/0953-8984/20/38/385209

Binding between endohedral Na atoms in Si clathrate I; a first principles study

H Tomono[1], H Eguchi[1,2] and K Tsumuraya[1]

[1] Department of Mechanical Engineering Informatics, School of Science and Technology, Meiji University, Kawasaki 214-8571, Japan
[2] Advanced Applied Science Department, Research Laboratory, IHI Corporation, Yokohama 235-8501, Japan

E-mail: abinitio[atmark]isc.meiji.ac.jp (K Tsumuraya)

Received 30 June 2008, in final form 31 July 2008
Published 27 August 2008
Online at stacks.iop.org/JPhysCM/20/385209

Abstract

We investigate the binding nature of the endohedral sodium atoms with the density functional theory methods, presuming that the clathrate I consists of a sheaf of one-dimensional connections of Na@Si_{24} cages interleaved in three perpendicular directions. Each sodium atom loses 30% of the $3s^1$ charge to the frame, forming an ionic bond with the cage atoms; the rest of the electron contributes to the covalent bond between the nearest Na atoms. The presumption is proved to be valid; the configuration of the two Na atoms in the nearest Si_{24} cages is more stable by 0.189 eV than that in the Si_{20} and Si_{24} cages. The energy of the beads of the two distorted Na atoms is more stable by 0.104 eV than that of the two infinitely separated Na atoms. The covalent bond explains both the preferential occupancies in the Si_{24} cages and the low anisotropic displacement parameters of the endohedral atoms in the Si_{24} cages in the [100] directions of the clathrate I.

(Some figures in this article are in colour only in the electronic version)

1. Introduction

The understanding of the mechanism of cohesion of condensed matter is essential for solid state physics. Silicon clathrates are compounds with endohedral atoms in the cages of the host frame network and expanded phases of diamond type silicon crystal. Cros *et al* [1] inspired by the structure of the clathrate natural gas hydrates, first synthesized silicon clathrate I containing Na atoms. Group 14 clathrate I has been successively synthesized only when alkaline [2–4] or alkaline earth metal atoms [5] or Cl, Br, or I in group 17 atoms [6] are encapsulated into the clathrate cages. The electro-negativity differences between these host and guest atoms are smaller than those in the ionic crystals. If the host and guest atoms have large differences, then the induced electron transfer forms ionic compounds with simple structures like NaCl or CsCl type structures.

To date we have found few reports on the role of the endohedral atoms in the cohesion of the group 14 clathrates. The electron charge transfers, from the endohedral Na atom to the frame silicon atoms, were predicted in clathrate I [7, 8] and a partial transfer in a Ba@Si_{20} cluster [9]. In clathrate II, the displacement of the guest atoms was predicted to be 0.17 Å from the center of the Si_{28} cage and explained as due to a combination of the Jahn–Teller and Mott transition [10]. Brunet *et al* [11] observed the displacement using EXAFS (extended x-ray absorption fine structure) analysis. The Na atom was displaced away from the Si_{28} cage-center toward the center of a hexagonal ring by 0.9 ± 0.02 Å [11]. Libotte *et al* [12] calculated the displacements of the endohedral Na atoms in clathrate II and found the displacements to be 0.456 Å, from the *ab initio* calculation, and 0.91 Å, from a tight-binding calculation. Tournus *et al* observed the displacements to be 1 Å in the Si_{28} cage of clathrate II Na_2@Si_{34} and 2 Å in clathrate II Na_6@Si_{34} [13]. They also calculated the displacements of the Na atoms in the Si_{28} cage as 0.65 Å from the supercell calculation of the Na_2@$Si_{50}H_{44}$ cluster with a periodic DFT calculation. They proposed the possibility that the displacements were due to the Peierls or Jahn–Teller effect.

Recently one of the authors reported the displacements of the Na atoms in the two adjacent Si_{28} cages hydrogenated to terminate the dangling bonds of the Si atoms on the surface of the clusters [14]. Each Na atom was displaced by 0.63 Å away from the centers of their cages to form a dimer between

the endohedral Na atoms. The displacements was attributed to the formation of covalent bond between the endohedral Na atoms. They also found the electron charge transferred from the endohedral atoms to the silicon atoms.

So the following questions arise: what is the binding between the endohedral atoms in the cohesion of the clathrates? Why do the host–guest combinations not crystallize into simple ionic structures? In the following we use a first principles analysis to address the questions by investigating the guest–guest and the host–guest interactions in the clathrate I.

Figure 1 shows a schematic drawing of the polyhedral structure of the clathrate I. The structure is special in that it consists of the bamboo like Si_{24} cages only; the cages (white) are arranged in bamboos, with spacing a of lattice constant, in one-dimensional horizontal direction sharing hexagonal rings as the bamboo joints between the adjacent Si_{24} cages. Weaving the bamboos in three dimensions with common pentagonal surfaces forms voids shown with black polyhedron regions in figure 1. Each void is a pentagonal dodecahedron, separated in space, located at bcc position with a different orientation. All the previous papers identified the existence of the Si_{20} cages in the clathrate I. However we presume the structure consists of only Si_{24} cages; figure 1 shows that Si_{20} cages are merely accidental voids in the weaved bamboos in the three dimensions. The voids just correspond to α cages in zeolites, although the voids in the clathrate I are far smaller than the ones in the zeolites. The accidental voids are predicted to play a minor role in the cohesion of the clathrate I. Although this view on the clathrate I structure has been neglected so far, the experimental preferential occupancies of the endohedral atoms in the Si_{24} cages [15–17] and the experimental anisotropic displacement parameters support this bamboo model.

So presuming the clathrate I as consisting of the bamboo structures in three perpendicular directions, we analyze the bonding nature between the endohedral atoms in the clathrate. First, we calculate the relaxed geometries of the one-dimensional clusters with different numbers of Si_{24} cages using the real-space DFT method and show the binding nature between the guest atoms; the dimer formation is due to the covalent bonding between the adjacent endohedral Na atoms and the charge transfer from the Na atoms to the cage atoms. Next, we evaluate the cohesion energy of the chained Na atoms using the periodic DFT method.

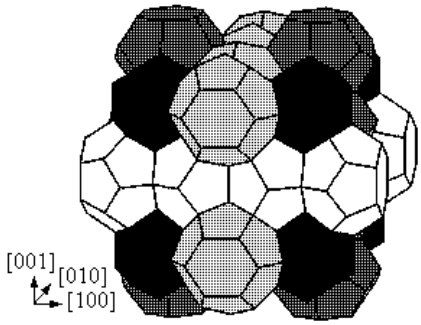

Figure 1. Polyhedron structure of the clathrate I Si_{46} by extending the simple cubic unit cell. Two horizontal white bamboos of the polyhedron are a one-dimensional bamboo like connection of the tetradecahedron (Si_{24}) cages in the [100] direction. The connections, arranged in three perpendicular directions with spacing a of lattice constant, forms the black voids of the pentagonal dodecahedron. This structure is the clathrate I Si_{46}, free of endohedral atoms, consisting of the tetradecahedra only.

2. Computational details

We perform the real-space DFT calculation for the hydrogenated bamboo structures using the generalized gradient approximation of Perdew, Burke and Ernzerhof (GGA-PBE) [18]. We use the frozen core $1s^2 2s^2 2p^6$ approximation for the Na and the silicon atoms and atomic orbitals with the valence $3s^1$ orbital for the Na atom and the valence $3s^2 3p^2$ orbitals for the silicon atom for which we use double atomic functions for each orbital. No smearing for occupations is applied to the final geometrical optimization. Since we regard the bamboo clusters as representing the essential aspects of the clathrate I, we add hydrogen atoms to the three coordinated silicon atoms on the surface of the bamboo structures, to mimic both the electronic density of states (DOS) and the bonding configurations in the clathrate I with the clusters. The hydration on the surface of clusters mimics almost the same electronic states as in the crystalline clathrates. The calculated displacements [13, 14] in the hydrogenated double Si_{28} cages in the clathrate II coincided with, not only the experimentally observed displacements 0.9 Å [11] or 1 Å [13], but also the calculated displacements 0.456 Å [12] or 0.91 Å [12] in the crystalline clathrates II. This hydration enables the states of the dangling bonds on the surface of the bamboo structure to shift to the lower side in energy as will be shown in figure 4. This hydration realizes the same features as in the DOS of the clathrate $Ba_8@Si_{46}$ [19]. We use an ADF code [20, 21], which uses a linear combination of Slater type orbitals. To evaluate the cohesion energy of the chain of the two endohedral Na atoms in the clathrate I, we use a periodic DFT code PHASE [22] with the norm conserving pseudopotentials for the Na ($3s^1$) and Si ($3s^2$ and $3p^2$) pseudoatoms. For the periodic DFT calculations, Brillouin zones are sampled at the $\mathbf{\Gamma}$ and $\mathbf{X}$ point set. Markov, Shah and Payne have shown that this set is an efficient $\mathbf{k}$-point set to remove defect interactions in the periodic cells [23]. The numbers of plane waves are kept 13 805 at the $\mathbf{\Gamma}$ point and 16 184 at $\mathbf{X}$ for any lattice constant. It corresponds to setting the cutoff energy to be 20.0 Ryd (272.11 eV) at 11.0 Å. We use the PBE [18] exchange and correlation functionals for the electron correlations for the periodic DFT calculations. We use the spin unrestricted calculations for both the real-space and the periodic calculations with the convergence of interatomic forces reduced to below 9.45×10^{-3} H Å^{-1} (5.0×10^{-3} H/bohr).

3. Results

The distances between the endohedral Na atoms in the relaxed four-caged bamboo structure $Si_{78}H_{60}$ are shown in figure 2(a) as an example of the relaxed structures of an even number of cage clusters. Although the distances between the hexagonal rings are almost constant, the inter-Na distances A and C are,

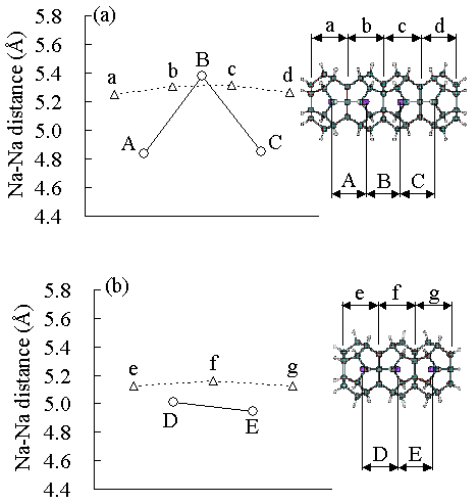

Figure 2. The inter-Na distances of (a) four-caged $Na_4@Si_{78}H_{60}$ bamboo cluster and (b) three-caged $Na_3@Si_{60}H_{48}$ cluster, where the triangles △ are the inter-hexagonal distances in the bamboo structures. The lines (—— and · · · · · ·) are for visual guidance.

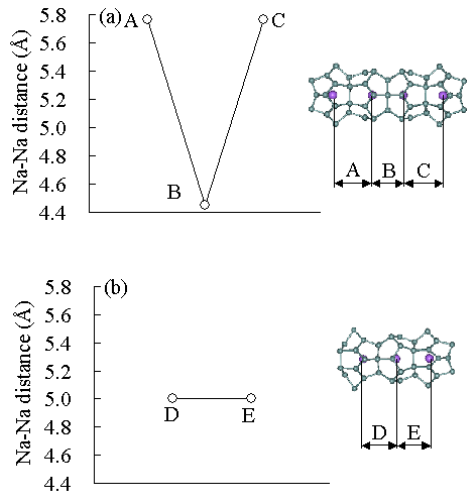

Figure 3. The inter-Na distances of (a) the four-caged $Na_4@Si_{78}$ bamboo cluster and (b) the three-caged $Na_3@Si_{60}$ cluster. The line is for visual guidance.

however, shorter than the inter-hexagonal distances: the inter-Na distances *A* (4.84 Å) and *C* (4.85 Å) at the ends of the bamboo structure are shorter than the distance *B* (5.38 Å). The short distances are induced by a bonding between the Na atoms. The sum of the shorter and the longer distances is 10.21 ∼ 10.23 Å which almost equals the experimental lattice constant 10.19 ± 0.02 Å of clathrate I $Na_8@Si_{46}$ [24]. We show the distances in the three-caged $Na_3@Si_{60}H_{48}$ cluster in figure 2(b) as an example of an odd number of the cages. The inter-Na distances, which are smaller than the ones between the adjacent hexagonal rings, are almost the same for each endohedral atom. A balance of forces exists between the central Na atom and the adjacent two Na atoms. So the small inter-Na distances *A* and *C* in figure 2(a) are induced by the dimer formation between the Na atoms. The formation may lead to a Peierls distortion in the bamboo clusters.

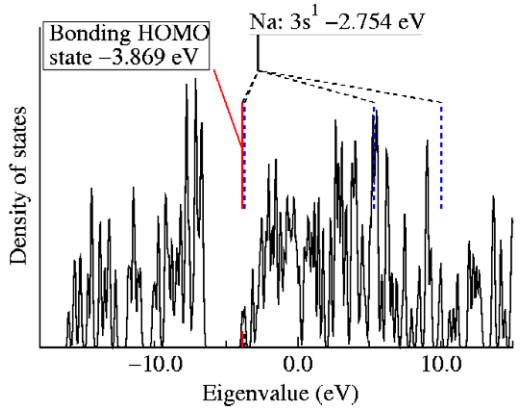

Figure 4. Molecular density of states (DOS) of the double-caged $Na_2@Si_{42}H_{36}$ cluster. The 3s state of the isolate Na atom splits into the bonding HOMO state and several unoccupied anti-bonding states.

For the Peierls distortion of the one-dimensional case with a free boundary condition, the inter-atom distances at the edge are different from those in a periodic boundary condition. Since two neighbor atoms at the edges form an edge state in the Peierls gap [25], their distances are longer than the ones of the inner inter-atom bonding since they are located at the free boundary edge. The present bamboo structures have the free boundary condition. Thus the Si–H bonds at the edges do form longer Si–H bond distances. The Na atoms just inside the bonds in the four-caged structure form dimers with their adjacent inner Na atoms as shown *A* or *C* in figure 2(a). The same situation occurs for the three-caged cluster in figure 2(b). Here both the atoms forming the distances *D* and those forming the distance *E* try to form dimers. However they are balanced in force. Thus the length *D* is almost equal to that of *E*.

The distances between the endohedral Na atoms in hydrogen free four-caged bamboo structure Si_{78} are shown in figure 3(a). A single dimer exists at the center of the bamboo structure. Since both the Na atom pairs at the edges form the edge state with the relaxed longer distance, the Na atoms just inside the bond form the dimer. Figure 3(b) shows the distances between the endohedral Na atoms in the hydrogen free three-caged bamboo structure Si_{60}. The inter-Na distances are the same for each endohedral atom; a balance of forces exists between the central Na atom and the adjacent two Na atoms. These figures 2 and 3 indicate that the Peierls distortion exists between the endohedral Na atoms in these bamboo structures.

Figure 4 shows the molecular DOS of the double-caged $Na_2@Si_{42}H_{36}$ cluster. The shape of the earlier density of states [26, 27] of the clathrate are similar to this density of states. The HOMO state is at −3.869 eV and the LUMO is at −3.703 eV, where HOMO is the highest occupied state and LUMO is the lowest unoccupied state. The HOMO–LUMO gap is 0.166 eV. The magnitude of the LDA gap was 0.177 eV with the electron correlation by Vosko *et al* [28]. No experimental band gap energy is given, since HOMO is located at just above the gap. The eigenvalue −2.754 eV for the 3s state of the isolate Na atom splits into an occupied single bonding state −3.869 eV (18A1.g) which is the HOMO

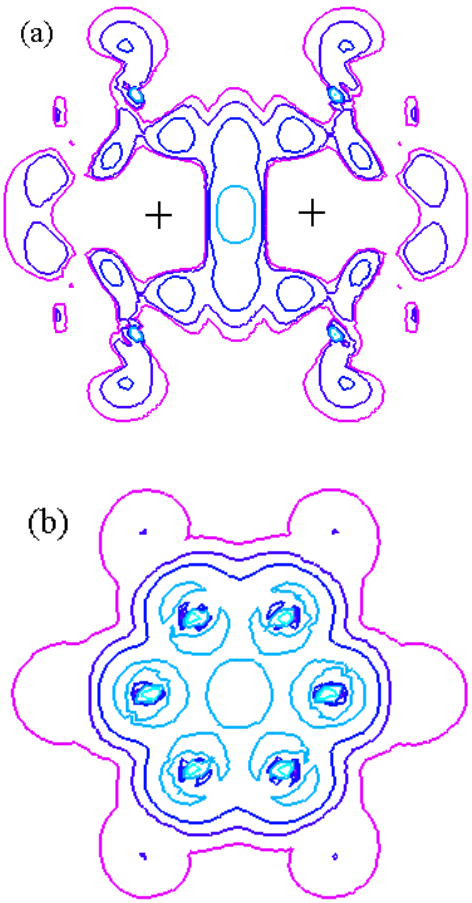

Figure 5. The spin unrestricted difference electron charge density profiles $\Delta\rho_{\mathrm{Na–Na}}$ given by (1), where the densities are plotted on a logarithmic scale, $10^{-5} \times 10^{5N/10}$ e Å^{-3}, $N = 0$–10. The blue lines are higher densities than the purple ones. The two plus marks correspond to the positions of the endohedral Na atoms. The blank regions correspond to the densities that are negative or less than 10^{-5} e Å^{-3}. The density (a) is shown on the plane that intersects the two endohedral Na atoms and the midpoint between two Si atoms on the hexagonal ring shared by the adjacent two Si_{24} cages. The density (b) on the hexagonal ring between the two adjacent Na atoms in the Si_{24} cages.

state and several higher anti-bonding states 16B3.u (LUMO, −3.703 eV), 28A1.g (5.328 eV) and 26B3.u (10.02 eV). The decrease of the eigenvalue from the 3s at −2.754 eV to the HOMO edge at −3.869 eV is due to the formation of the bonding state between the endohedral atoms. This is just the bonding state formation in hydrogen molecule. Since the HOMO 18A1.g state is composed of a 'gerade' function, the corresponding electron state gives an even function with respect to the center of the molecule. There is a large forbidden region from the HOMO down to the state 9A1.u at −6.593 eV indicating the cluster is an insulator with HOMO–LUMO gap 2.724 eV, if the double-caged cluster has no endohedral atom. For the four-caged bamboo structure, the HOMO–LUMO gap was 0.255 eV. This corresponds to a Peierls gap in this cluster.

To examine the bonding electron distribution between the endohedral Na atoms in the double-caged cluster, we show the

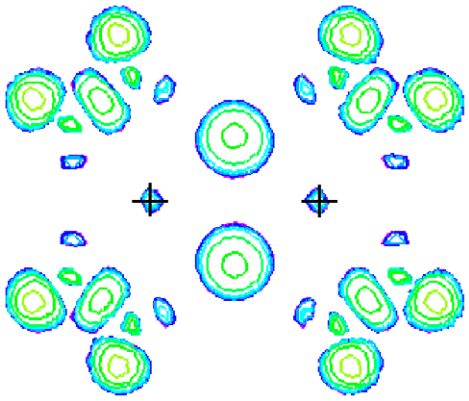

Figure 6. The difference charge density between the converged self-consistent electron and the overlapped isolated atom density. The densities are plotted on the same plane as in figure 5(a) with a logarithmic scale, $10^{-5} \times 10^{5N/10}$ e Å^{-3}, $N = 0$–10. The green contours are higher than the purple ones. The blank regions are lower than 10^{-5} e Å^{-3} including negative densities.

electron density profile in figure 5 given by

$$\begin{aligned}\Delta\rho_{\mathrm{Na–Na}} &= (\,\mathrm{Na\ Na}\,) + (\,\circ\ \circ\,) - (\,\mathrm{Na}\ \circ\,) - (\,\circ\ \mathrm{Na}\,) \\ &= \rho(\mathrm{Na_2@Si_{42}H_{36}}) + \rho(\mathrm{Si_{42}H_{36}}) \\ &\quad - \rho(\mathrm{Na@Si_{42}H_{36}}) - \rho(\mathrm{Na@Si_{42}H_{36}}), \end{aligned} \tag{1}$$

where open circles represent the vacancies of the endohedral Na atoms. The coordinates of the last three terms are fixed at those of the first term to obtain the difference of the electron charge densities. This expression gives the interaction electron density between the Na atoms, since the net number of atoms is canceled. We used the spin polarized calculations for all the terms; the non-spin states were the lowest for the first two terms and the spin states with $\mu_{\mathrm{B}} = 1$ were the lowest for the last two terms. We evaluated the sum of the up-spin density and the down-spin density for each structure and substituted them into the above equation; the density distribution is shown in figure 5(a). This figure shows a clear covalent bonding density between the Na–Na bond. This is formed by the dimer formation. The density is due to the bonding state between each $3s^1$ valence electron in the two Na atoms; this is just like the covalent bond formation between two hydrogen atoms. We show in figure 5(b) the difference density on the hexagonal ring located at the bisector plane between the two plus marks in (a). There is a finite covalent charge density on the plane. Neither the total electron density nor the partial charge density due to the HOMO state in figure 4 shows this type of the covalent bond charge density between the Na atoms. The densities of the bonding states appeared between the dimers in the even number of cages.

To see the spatial distribution of the electron transfers around the endohedral atoms, we show in figure 6 the difference electron density profile

$$\Delta\rho = \rho_{\mathrm{opt}} - \sum \rho_{\mathrm{atom}}, \tag{2}$$

where ρ_{opt} is the density of the geometrically optimized cluster and ρ_{atom} is the overlapped density of the isolated constituent atoms. The blank zone corresponds to regions with lower

densities than 10^{-5} e Å^{-3} or with negative densities. So the contour lines correspond to the increased charge ones compared to the overlapped isolated atom densities. The electrons around the endohedral Na atoms are depleted to the cage silicon atoms except for the nucleus positions of the Na atoms.

We calculate electron transfers from the endohedral Na atom to the frame atoms. There are several methods to calculate the transfer. Among them the Mulliken charges have been found to depend on a number of linear combinations of atomic orbitals for the basis functions [29]. Voronoi charges, which were named as Voronoi deformation charge VDC, have been found to give reasonable values for the transfer [29]. The transferred $3s^1$ electron from each endohedral Na atom to the frame silicon atoms were $0.320e$ for the double-caged bamboo structure. The ionic states also appeared in the triple-caged bamboo structure: the electron transfers from Na atoms to frame atoms were $0.343e$ (middle Na atom) and $0.297e$ (edge Na atoms) for the triple-caged bamboo cluster showing that the remaining $3s^1$ electron of the endohedral Na atoms formed the covalent bonding state between the endohedral Na atoms as shown in figure 5.

Here we evaluate the cohesion energy of the Na chain in the clathrate I. For this purpose we evaluate the energy using the periodic DFT method with the same type equation as (1);

$$E^{\mathrm{c}} = \boxed{\mathrm{Na}\quad\mathrm{Na}} + \boxed{\phantom{\mathrm{Na}\quad\mathrm{Na}}} - \boxed{\mathrm{Na}} - \boxed{\mathrm{Na}}$$
$$= E_{\mathrm{T}}(\mathrm{Na_2@Si_{46}}) + E_{\mathrm{T}}(\mathrm{Si_{46}}) - E_{\mathrm{T}}(\mathrm{Na@Si_{46}}) - E_{\mathrm{T}}(\mathrm{Na@Si_{46}}), \quad (3)$$

where E_{T}'s are the total energies of each crystal. The net number of each kind of atom is also canceled in this equation. The last two terms correspond to each Na atom being located at infinitely separated positions in the clathrate. Therefore this equation enables us to evaluate the cohesive energy of the Na chain in the clathrate I. The equation was derived from the difference of the formation energies of each phase by Sawada *et al* [30]. They proposed this equation to evaluate the binding energies between the substitutional solute atom and the interstitial solute atom in the bcc iron. They needed to maximize the energy in the supercells. For our calculation the use of the unit cell is sufficient, since we need to calculate the cohesion energy of the Na chain in the clathrate. We calculate four kinds of equation of states for each clathrate in (3). Here we have assumed the energies of the last two terms to be equivalent due to their symmetry. The equation used is

$$E^{\mathrm{c}} = E_{\mathrm{T}}(\mathrm{Na_2@Si_{46}}) + E_{\mathrm{T}}(\mathrm{Si_{46}}) - 2E_{\mathrm{T}}(\mathrm{Na@Si_{46}}). \quad (4)$$

The energy of the first term was the lowest for a spin polarized state $\mu_{\mathrm{B}} = 0.188$ and the other terms for the non-spin states. The equilibrium lattice constant of this clathrate was 10.1998 Å, the shorter inter-Na distance was 5.0915 Å, and the longer one 5.1083 Å, showing a difference of 0.0168 Å in the [100] direction. The difference between these two distances is smaller than that in the hydrogenated cluster in figure 2(a). This is because of the infinite chain connection of the Na atoms in the clathrate I. The cohesive energy E^{c} of the chain was 0.104 eV which is finite and attractive, so the chain is more stable than the two infinitely separated Na atoms in the clathrate I.

To evaluate the energy gain of the distortion in the crystalline state, we calculate the total energy of the clathrate in which the two Na atoms are located at the centers of the gravity of the nearest Si_{24} cages of the first term in (4). This energy was higher by 0.001 86 eV, with the shorter inter-Na distance 5.0978 Å, than the full relaxed clathrate. The shorter inter-Na distance in the full relaxed clathrate is shorter by 0.0062 Å than the inter-gravity distance. This quantity is a significant difference in the accuracy of the DFT calculations. This also indicates the existence of the attractive interaction between the shorter Na atom pairs.

4. Discussion

The endohedral atoms interacted with the cage atoms through the ionic bond and with the nearest endohedral atoms through the covalent bond.

We assumed that the clathrate I consists of the bamboo structures in the three perpendicular directions. Here, we examine the validity of this assumption. We calculated the total energy of the clathrate $Na_2@Si_{46}$ in which one of the two Na atoms is located in the Si_{20} cage and the other in the tSi_{24} cage. We have already calculated the energy of the clathrate $Na_2@Si_{46}$ in which two Na atoms are located at the nearest Si_{24} cages. The energy is given by the first term in (4). The energy of this clathrate is more stable by 0.189 eV than that of the former clathrate; the bond between the two Na atoms in the chain is more stable than the two Na atoms in the Si_{20} and Si_{24} cages. This is further evidence of the validity of our presumption for the structure of the clathrate I.

The covalent bond charge exists in figure 5 between the endohedral Na atoms. The validity of our bamboo structure model for the clathrate I is supported by experimental evidence of the preferential occupation of the Ba atoms in the Si_{24} cages by Yamanaka *et al* [16]. They reported that the Ba atoms occupy 0.985 of the six Si_{24} cages and only occupy 0.189 of the two Si_{20} cages. The high occupancy is a proof of the existence of the covalent bond between the Ba atoms Si_{24} cages. No explanation has yet been given for the origin of the occupancies.

The present study predicts the difference of the inter-Na distances to be only 0.0168 Å in the [100] direction. No report has been given for the experimental guest displacement in the clathrate I except for the guest displacement parameters [31, 32]. This is because the displacement is too small to be measured.

The anisotropy of the atomic displacement parameters of the endohedral atoms in clathrate I was reported by Chakoumakos *et al* [33, 34], Nolas *et al* [35] in which much smaller amplitudes in the [100] direction were reported than in the perpendicular direction. The present study explains the anisotropy as due to the constraint of the displacements of the Na atoms in the [100] direction induced by the covalent bond: the bond constrains the displacements between the nearest

Na atoms in the directions. No explanation is given for the origin of the anisotropies.

The covalent bond between the endohedral Na atoms prevents the atoms from crystallizing into ordered ionic structures like NaCl or CsCl and crystallizes into the caged clathrate structures. The bond forms beads of Na atoms in the clathrate I or a three-dimensional network of the Na atoms with T_d symmetry in the clathrate II. This is because the electro-negativity of the host 14 group atoms is smaller than that of the halogen atoms that crystallize into ionic crystals. The smaller electro-negativity differences between the host and guest atoms allow the guest Na atoms to form both covalent bonds between the guest atoms and ionic bonds through the charge transfer to the cages. Thus the clathrates are a compromised electronic state between ionic crystals and covalent crystals.

5. Conclusions

Presuming that the clathrate I consists of the sheaf of one-dimensional connections of Na@Si_{24} cages interleaved in three perpendicular directions, we investigated the binding nature of the endohedral Na atoms with both real-space and periodic DFT methods. Each Na atom has lost 30% of the $3s^1$ charge to the frame. A finite covalent bonding charge due to the Peierls distortion exists between the endohedral Na atoms in the caged clusters. The cohesion energy was 0.104 eV for the chain in the [100] directions of the clathrate I. The presumption was proved to be valid; the clathrate encapsulating two Na atoms in the [100] direction was more stable by 0.189 eV than the clathrate encapsulating the two atoms in the Si_{20} and Si_{24} cages. This covalent bond explains the experimental anisotropic displacement parameters and the preferential occupancies of the endohedral atoms in the Si_{24} cages of the clathrates I. The difference between the Na–Na distances was 0.0168 Å. This small magnitude of displacement explains the absence of experimental reports on the guest displacements in the clathrate I. The beads of the endohedral Na atoms in the directions are due to the covalent bond between the endohedral atoms accompanying the electron charge transfer from the endohedral atoms to the cages. The covalent bond explains both the preferential occupancies of the endohedral atoms and the low anisotropic displacement parameters in the [100] directions in the Si_{24} cages of the clathrate I. The beads are just a precipitated state in the regular solution theory. The smaller electro-negativity of group 14 host atoms than the halogen atoms allows the endohedral Na atoms to prevent atoms crystallizing into ionic crystals and allows the atoms to form covalent bonds with beads of endohedral atoms.

Acknowledgments

Computations were performed in part using SCore systems at the Information Science Center in Meiji University and Altix 3700 BX2 at YITP in Kyoto University.

References

[1] Cros C, Pouchard M and Hagenmuller P 1965 *C. R. Acad. Sci* **260** 4764
[2] Bobev S and Sevov S C 2000 *J. Solid State Chem.* **153** 92
[3] Gryko J, Mcmillan P F and Sankey O F 1996 *Phys. Rev.* B **54** 3037
[4] Nolas G S, Ward J M, Gryko J, Qiu L and White M A 2001 *Phys. Rev.* B **64** 153201
[5] Cordier G and Woll P 1991 *J. Less-Common Met.* **169** 291
[6] Reny E, Yamanaka S, Cros C and Pouchard M 2000 *Chem. Commun.* **24** 2505
[7] Zhao J, Buldum A, Ping Lu J and Fong C Y 1999 *Phys. Rev.* B **60** 14177
[8] Gatti C, Bertini L, Blake N P and Iversen B B 2003 *Chem. Eur. J.* **9** 4556
[9] Nagano T, Tsumuraya K, Eguchi H and Singh D J 2001 *Phys. Rev.* B **64** 155403
[10] Demkov A A, Sankey O F, Schmidt K E, Adams G B and O'Keeffe M 1994 *Phys. Rev.* B **50** 17001
[11] Brunet F, Mélinon P, Miguel A S, Kéghélian P, Perez A, Flank A M, Reny E, Cros C and Pouchard M 2000 *Phys. Rev.* B **61** 16550
[12] Libotte H, Gaspard J P, Miguel A S and Melinon P 2003 *Europhys. Lett.* **64** 757
[13] Tournus F, Masenelli B, Mélinon P, Connétable D, Blase X, Flank A M, Lagarde P, Cros C and Pouchard M 2004 *Phys. Rev.* B **69** 035208
[14] Takenaka H and Tsumuraya K 2006 *Mater. Trans.* **47** 63
[15] Cros C, Pouchard M, Hagenmuller P and Kesper J S 1968 *Bull. Chim. Fr.* **7** 2737
[16] Yamanaka S, Kawaji H and Ishikawa M 1996 *Mater. Sci. Forum* **232** 103
[17] Ramanchandran G K, McMillan P F, Dong J and Sankey O F 2000 *J. Solid State Chem.* **154** 626
[18] Perdew J P, Burke K and Ernzerhof M 1996 *Phys. Rev. Lett.* **77** 3865
[19] Kamakura N, Nakano T, Ikemoto Y, Usuda M, Fukuoka H, Yamanaka S, Shin S and Kobayashi K 2005 *Phys. Rev.* B **72** 14511
[20] Velde G Te, Bickelhaupt F M, Baerends E J, Guerra C F, Gisbergen S J A van, Snijders J G and Ziegler T 2001 *J. Comput. Chem.* **22** 931
[21] Painter G S, Ellis D E and Lubinsky A R 1971 *Phys. Rev.* B **4** 3610
[22] Katagiri H *et al* 2006 *RSS21 Free Software PHASE ver.5.00.* The Institute of Industrial Science, the University of Tokyo http://www.ciss.iis.u-tokyo.ac.jp/rss21/
[23] Makov G, Shan R and Payne M C 1996 *Phys. Rev.* B **53** 15513
[24] Cros C, Pouchard M and Hagenmuller P 1971 *Bull. Soc. Chim. Fr.* **2** 379
[25] Figge M T, Mostovoy M and Knoester J 2002 *Phys. Rev.* B **65** 125416
[26] Dong J and Sankey O F 1999 *J. Phys.: Condens. Matter* **11** 6129
[27] Madsen G K H, Schwarz K, Blaha P and Singh D J 2003 *Phys. Rev.* B **68** 125212
[28] Vosko S H, Wilk L and Nusair M D 1980 *Can. J. Phys.* **58** 1200
[29] Guerra C F, Handgraaf J W, Baerends E J and Bickelhaut E M 2003 *J. Comput. Chem.* **25** 189
[30] Sawada H, Kawakami K and Sugiyama M 2005 *Mater. Trans.* **46** 1140
[31] Paschen S, Carrillo-Cabrera W, Bentien A, Tran V H, Baenitz M, Grin Y and Steglich F 2001 *Phys. Rev.* B **64** 214404
[32] Christensen M, Bryan J D, Birkedal H, Stucky G D, Lebech B and Iversen B B 2003 *Phys. Rev.* B **68** 174428
[33] Chakoumakos B C, Sales B C, Mandrus D G and Nolas B C 2000 *J. Alloys Compounds* **296** 80
[34] Chakoumakos B C, Sales B C and Mandrus D G 2001 *J. Alloys Compounds* **322** 127
[35] Nolas G S, Weakley T J R, Cohn J L and Sharma R 2000 *Phys. Rev.* B **61** 3845